# Hierarchical Scheduling of Aggregated TCL Flexibility for Transactive Energy in Power Systems

Meng Song, Wei Sun, Yifei Wang, Mohammad Shahidehpour, *Fellow, IEEE*, Zhiyi Li, *Member, IEEE*, and Ciwei Gao

***Abstract*—This paper investigates a hierarchical approach to the optimal scheduling of flexibility offered as transactive energy by thermostatically controlled loads (TCLs). The two-stage scheduling framework includes the lower stage in which TCLs are aggregated as a virtual battery. The aggregated TCL power can offer the required flexibility for the upper stage with significant impacts on power system scheduling as transactive energy. Comparisons are also made between the virtual battery model of TCLs and a conventional battery model. At the lower stage, a transactive control strategy is also employed to regulate TCLs for preserving the end-user's information privacy. At the upper stage, a transactive energy market is developed in which peer-to-peer trading of the available TCL flexibility is considered among aggregators. Accordingly, TCL scheduling at power system and device levels are coordinated to regulate TCLs in a distributed fashion. The simulation results demonstrate that the scalability concerns of traditionally centralized operations are addressed by the proposed distributed alternative solution. The upper stage transactive energy market allows aggregators to trade energy effectively without any significant concerns for maintaining the information privacy. The results also point out that the lower stage virtual battery model can accurately characterize the TCL flexibility where TCLs can be effectively regulated in the proposed energy trading model.**

***Index Terms*—Transactive energy, thermostatically controlled loads, flexibility, electricity markets.**

Manuscript received June 4, 2019; revised October 6, 2019 and November 13, 2019; accepted November 21, 2019. Date of publication November 26, 2019; date of current version April 21, 2020. This work was supported in part by the Fundamental Research Funds for the Central Universities under Grant 2242019R20032 and in part by the U.S. Department of Energy under Award DE-EE0007998. Paper no. TSG-00787-2019. *(Corresponding authors: Yifei Wang; Mohammad Shahidehpour.)*

M. Song is with the School of Electrical Engineering, Southeast University, Nanjing 210096, China, and also with the ECE Department, University of Central Florida, Orlando, FL 32816 USA (e-mail: songmengseu@163.com).

W. Sun is with the ECE Department, University of Central Florida, Orlando, FL 32816 USA (e-mail: sun@ucf.edu).

Y. Wang and C. Gao are with the School of Electrical Engineering, Southeast University, Nanjing 210096, China (e-mail: wang-yf@foxmail.com; ciwei.gao@seu.edu.cn).

M. Shahidehpour is with the Robert W. Galvin Center for Electricity Innovation, Illinois Institute of Technology, Chicago, IL 60616 USA, and also with the Center of Research Excellence in Renewable Energy and Power Systems, King Abdulaziz University, Jeddah 23955, Saudi Arabia (e-mail: ms@iit.edu).

Z. Li is with the College of Electrical Engineering, Zhejiang University, Hangzhou 310027, China (e-mail: zhiyi@zju.edu.cn).

Color versions of one or more of the figures in this article are available online at http://ieeexplore.ieee.org.

Digital Object Identifier 10.1109/TSG.2019.2955852

## NOMENCLATURE

*Sets and Indices*

| | |
|---|---|
| $c$, $d$ | Indices for charging and discharging |
| $k$ | Index for time slot |
| $i(v)$, $j$ | Indices for aggregator (AGG) and TCL |
| $t$ | Index for time |
| $g$, $G$ | Indices for generator. |

*Parameter*

| | |
|---|---|
| $C_a$ | Equivalent thermal capacity (kJ/°C) |
| $COP$ | Coefficient of performance for TCLs |
| $T_{out}$ | External temperature (°C) |
| $P_{rated}$ | Rated electric power of a TCL (kW) |
| $R$ | Equivalent thermal resistance (°C/kW) |
| $T_{set}$ | Temperature set-point (°C) |
| $\delta$ | Temperature dead band width (°C) |
| $T_{min}$, $T_{max}$ | Minimum and maximum internal temperature of TCL (°C) |
| $\kappa$, $\gamma$ | Coefficient of TCL virtual battery |
| $\alpha$ | Coefficient of virtual battery for aggregated TCLs |
| $P_{min}$, $P_{max}$ | Minimum and maximum charging/discharging power of virtual battery for aggregated TCLs (kW) |
| $SOC_{min}$, $SOC_{max}$ | Minimum and maximum State of Charge (SOC) of virtual battery |
| $n$, $N_k$, $N_{agg}$ | Number of TCLs, time slots and aggregators, respectively |
| $\omega_1$, $\omega_2$ | Coefficients of bid price |
| $a$, $b$, $c$ | Coefficients of generator generation cost function |
| $d_{iv}$ | Equivalent electrical distance between aggregator $i$ and $v$ |
| $h$, $l$ | Parameters for Lagrangian multiplier update |
| $P^c$, $P^d$ | Maximum charging and discharging power of conventional battery (MW) |
| $\eta^c$, $\eta^d$ | Charging and discharging efficiency of conventional battery |
| $o$ | Capacity of conventional battery (MWh) |
| $soc_{min}$ $soc_{max}$ | Minimum and maximum state of charge of conventional battery |
| $soc_0$ | Initial state of charge of conventional battery. |

*Variables*

| | |
|---|---|
| $T_{in}$ | Internal temperature (°C) |
| $S$ | TCL status: $S$ is 1 if TCL is on; otherwise, $S$ is 0 |
| $P_{cont}$ | Electric power of continuous TCL power model (kW) |
| $P_{baseline}$ | Power baseline of TCL (kW) |
| $P_{cd}$ | Charging/discharging power of virtual battery for individual TCL (kW) |
| $x$ | State of charge of virtual battery for individual TCLs |
| $\Delta t$ | Time slot duration (second) |
| $SOC$ | State of charge of the virtual battery model for aggregated TCLs |
| $P$ | Charging/discharging power of the virtual battery for aggregated TCLs (kW) |
| $N_t$ | Number of total control signals |
| $N_r$ | Number of TCL enforced switching |
| $P_{desired}$ | Desired power of TCLs (kW) |
| $P_{actual}$ | Actual power of TCLs (kW) |
| $\Delta P$ | Power adjustment of TCLs (kW) |
| $\rho_1$, $\rho_2$ | Bid price components |
| $\rho_{pid}$ | Bid price for the virtual battery ($/kW) |
| $\rho_{pid}^{cl}$ | Market clearing price ($/kW) |
| $\rho$ | Contract price of AGG ($/MW) |
| $P_{G,i}$ | Power of generator owned by AGG $i$ (MW) |
| $P_{pur,iSO}$ | Power purchased by AGG $i$ from SO(MW) |
| $P_{pur,iv}$ | Power purchased by AGG $i$ from AGG $v$ (MW) |
| $P_{sel,i}$ | Power sold by AGG $i$ to other AGGs(MW) |
| $P_{battery,i}$ | Charging/discharging power of virtual battery owned by AGG $i$ (MW) |
| $P_{load,i}$ | Load of AGG $i$ (MW) |
| $m$ | Number of Lagrangian multiplier iterations |
| $\lambda$ | Lagrangian multiplier. |

## I. Introduction

THE VARIABILITY of distributed energy resources (DER) can increase the power supply deficiency and culminate in a critical condition as DER proliferation continues to escalate in power systems [1]. Traditionally, thermal generators and energy storage devices were employed to compensate such deficiencies [2]. However, frequent power adjustments could increase the power system operation cost and place additional stress on thermal power generators as variability increases [3]. Thermostatically controlled loads (TCLs), such as water heaters, refrigerators, and air conditioning units, can serve as indispensable demand response (DR) resources. They are progressively utilized to address DER variability quickly, economically and effectively [4]. TCLs possess thermal inertia and have attracted additional attention to participate in power system operations. However, TCL's specific properties pose a key challenge to effectively participate in the power system scheduling and control.

First, it would be difficult to schedule TCLs individually as their adjustable capacities are too small to have significant impacts on power systems [5]. Also, the number of TCLs could traditionally be very large, which would require significant computation resources when TCLs are individually scheduled. Accordingly, TCL aggregation is required for their participation in power system operations. Meanwhile, TCLs with thermal inertia act like batteries which provide various grid services owing to their flexible charging and discharging capabilities [6]. References [7] and [8] proposed a stochastic battery model for representing the aggregated TCL flexibility with a concise collection of power signals. Reference [9] developed a rough time-varying thermal energy storage model to denote the aggregated TCL flexibility in which suboptimal control trajectories were calculated. In [10], a leaky storage unit was proposed to embody the aggregated flexibility of TCLs in the optimization of multiservice portfolios. A generalized battery model that described flexibilities of TCLs and conventional batteries for delivering power grid and end-use services was presented in [11]. A virtual battery model of HVAC was also studied in [12]. TCLs show great potentials in terms of virtual energy storage which can replace conventional batteries to serve the power grid. Nevertheless, differences between the battery model of aggregated TCLs and conventional batteries are seldom highlighted, which need to be investigated further for the provision of TCLs and conventional batteries in power system operations.

Second, widespread TCLs throughout a power network are often regulated in a centralized fashion. For example, [10] conducted a linear optimization model of TCLs for frequency and energy arbitrage. A hierarchical centralized load control with TCLs was proposed in [13] to provide load following services. In [14], a sequential setpoint control of TCL population was provided in which aggregated TCLs were characterized by an extended Markov model. However, a centralized TCL operation is more complicated which could expose TCLs' information privacy [15], [16]. In practice, a distributed scheduling and control is more practical for regulating largely distributed TCLs which can protect the corresponding information privacy effectively.

Transactive control that employs market mechanisms to enable self-interested entities to serve the power grid, is a promising distributed way to preserve the proprietary data and respect specific performances of participating entities [17]. Reference [18] proposed a real-time electric vehicle (EV) charging management scheme in a transactive energy market. EV owners provide charging requirements and price signals, while end-users' information privacy is preserved. A day-ahead transactive market framework was presented in [19] in which transactive energy in transmission and distribution networks was cleared simultaneously for optimal operations of distributed resources. The clearing process for trading in a transactive energy market was studied in [16], [20]. Here, Lagrangian relaxation was introduced to describe the trading process. Reference [16] proposed an optimal strategy for multi microgrids using dynamic programming. Reference [20] developed a distributed optimization framework by Lagrangian relaxation for energy trading among microgrids. Transactive control provided an innovative solution to regulate TCLs in a distributed fashion; however, additional investigations are required to fully explore the stated potentials.

Additional studies focused on TCL regulation by transactive control. Reference [21] provided a framework for transaction-based building controls. Reference [22] proposed a single-auction market for commercial buildings to respond to external price signals. Each building provides a price curve for adjusting its temperature set-point. In [23], a transactive control strategy was developed for regulating commercial buildings to shave power peaks and shift loads. In this case, building bidding strategies and market clearing process were both provided. The device bidding and market clearing strategies were investigated in [24], [25] to motivate self-interested TCLs to pursue efficient energy allocations at peak hours, in which TCLs were regulated by a market-based coordination framework. The transactive control of residential building was analyzed in [26]. Even though the transactive TCL control was analyzed earlier at the level of devices/buildings, the optimal scheduling of aggregated TCLs was rarely analyzed at the power system level. Moreover, specific TCL performances in transactive control (i.e., lockout time effects) were often disregarded.

In this paper, we focus on a hierarchical optimal scheduling and control of TCL populations in power systems using market-based distributed modes. Accordingly, specific operating characteristics of TCLs will be fully considered and participants' information privacy will be preserved. The main contributions of this paper are summarized as follows. First, a hierarchical framework is proposed for TCLs, in which the TCL scheduling at power system and device levels are coordinated to regulate TCLs in a distributed fashion. At the lower stage, a virtual energy market is designed to control TCLs at the device level in which specific TCL characteristics are fully considered. At the upper stage, a transactive energy market is adopted for aggregated TCLs in which the proposed peer-to-peer optimal trading strategy among aggregators would minimize the cost of power system operation. Each aggregator makes proper decisions according to other aggregators' trading signals without revealing any private information. Second, based on the virtual battery model for the provision of aggregated TCL flexibility, the paper investigates the differences among virtual and conventional battery models in terms of operating behaviors.

The paper is structured as follows. TCL scheduling framework is described in Section II. Aggregation and de-aggregation of TCLs are given in Section III. Section IV describes transactive energy market operation with aggregated TCL flexibility. Case studies developed in Section V. Section VI concludes the paper.

## II. TCL Scheduling Framework

The hierarchical framework for distributed TCL scheduling is shown in Fig. 1. In this paper, TCLs connected to a power network node are regulated by an aggregator [27]. The implementation procedure is summarized as follows. As TCLs are widely distributed in the grid, they are aggregated as a virtual battery model at the lower stage (aggregating/de-aggregating) to qualify their system scheduling potential (see Section III-A). When aggregators receive the virtual battery model of TCLs, each aggregator (AGG) uses the aggregated data of

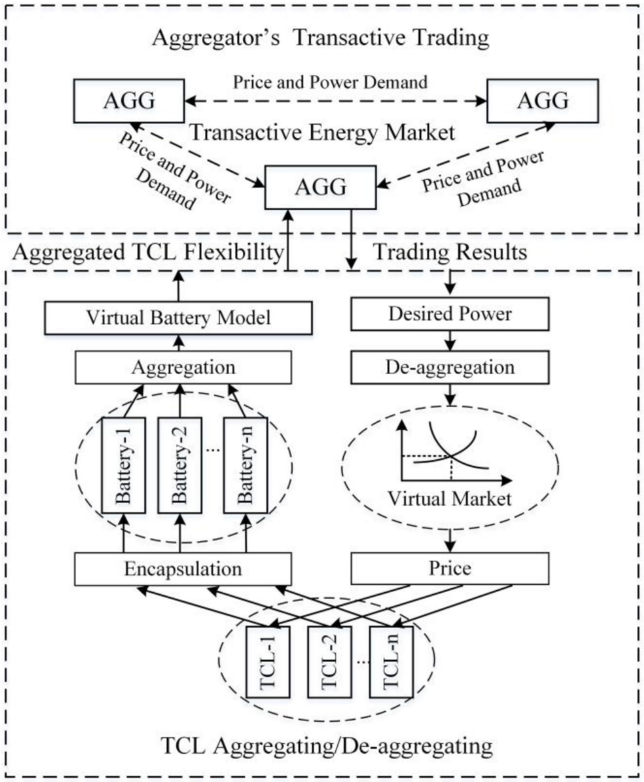


Fig. 1. Hierarchical TCL scheduling framework.

TCL flexibility to participate in a transactive energy market at the upper stage (aggregator's transactive trading, see Section IV). System-level peer-to-peer trading among aggregators with aggregated TCLs is to minimize the power system cost.

TCLs are controlled in a distributed fashion by hosting a virtual market at the lower stage as aggregators receive transactive results from the upper stage (see Section III-B). Each TCL determines its own operating state in terms of its bid and market clearing price. Accordingly, TCLs are optimally regulated in a distributed fashion by the coordination of system- and device level schedules.

The virtual battery model is employed to characterize the aggregated TCL flexibility, which guarantees that the virtual battery is scheduled at the upper stage to reside within TCL capabilities stated at the lower stage. Also, eligible TCLs are regulated by aggregators to respond to the desired power at the lower stage (see Section III-B). The proposed hierarchical framework allows TCLs at the lower stage to follow the aggregated TCLs' power scheduled at the upper stage.

## III. Aggregation and De-Aggregation of TCLs

### A. Aggregation of TCLs at the Lower stage

There are two operating modes (i.e., heating and cooling) for certain TCLs (e.g., air conditionings) and cooling mode is presented as an example in this paper. The thermodynamic behavior of TCLs is described by a discrete equivalent model [9], [13], and [28], which is given as:

$$C_a \frac{dT_{in}(t)}{dt} = \frac{T_{out} - T_{in}(t)}{R} - S(t) \cdot COP \cdot P_{rated} \quad (1)$$

TCLs working at the rated power (on state) or zero power (off state) have their indoor temperatures adjusted periodically within $[T_{\min}, T_{\max}]$ ($T_{\min} = T_{\text{set}} - \delta, T_{\max} = T_{\text{set}} + \delta$) [29]. A continuous TCL model for closely following the aggregated TCL power is proposed in [7]. The continuous model, utilized as a more convenient choice than the discrete equivalent model, describes the TCL performance as:

$$C_a \cdot \frac{dT_{in}(t)}{dt} = \frac{T_{out} - T_{in}(t)}{R} - COP \cdot P_{cont}(t) \tag{2a}$$

$$0 \le P_{cont}(t) \le P_{rated} \tag{2b}$$

When there are no external control signals, TCL operates at $T_{set}$ with the corresponding baseline power, $P_{baseline}$, expressed as:

$$P_{baseline} = \frac{T_{out} - T_{set}}{COP \cdot R} \tag{3}$$

TCLs have thermal inertia and share similar operating behaviors with batteries. Accordingly, TCL operation is presented as a virtual battery model in this paper. When there are external control signals, the TCL power $P_{cont}(t)$ will be changed and the internal temperature will deviate from $T_{set}$. If $P_{cont}(t)$ is larger than $P_{baseline}$, TCL absorbs power from the grid to store energy in virtual battery. Otherwise, TCL releases power to the grid by discharging the energy stored in virtual battery. Thus, the difference between $P_{cont}(t)$ and $P_{baseline}$ is defined as the charging/discharging power of virtual battery, which is stated as:

$$P_{cd}(k) = P_{cont}(k) - P_{baseline} \tag{4a}$$

$$-P_{baseline} \le P_{cd}(k) \le P_{rated} - P_{baseline} \tag{4b}$$

When $T_{\text{in}}(t)$ is at $T_{\max}$ or $T_{\min}$, the stored energy is either the lowest or the highest, respectively. Considering that $T_{\text{set}}$ is the user's preferred temperature setpoint, its corresponding energy storage is set at 0 in this paper. Thus, energy storage is defined as:

$$x(k) = \frac{T_{set} - T_{in}(k)}{\delta} \tag{5}$$

where, $T_{\text{in}}(k)$ is within $[T_{\min}, T_{\max}]$ to guarantee end-users' comfort. Thus, $x(k)$ is constrained as:

$$-1 \le x(k) \le 1 \tag{6}$$

Using (2a), (3), (4a) and (5), the updated TCL energy storage level is derived as:

$$x(k+1) = \kappa x(k) + \gamma P_{cd}(k) \tag{7a}$$

where

$$\kappa = \exp\left(-\frac{\Delta t}{RC_a}\right) \tag{7b}$$

$$\gamma = \frac{COP \cdot R \cdot (1-\kappa)}{\delta} \tag{7c}$$

Accordingly, TCL is encapsulated in a battery model using (4b), (6) and (7a). TCL energy storage levels are presented as:

$$\begin{cases} x_1(k+1) = \kappa_1 x_1(k) + \gamma_1 P_{cd,1}(k) \\ x_2(k+1) = \kappa_2 x_2(k) + \gamma_2 P_{cd,2}(k) \\ \qquad\qquad \vdots \\ x_n(k+1) = \kappa_n x_n(k) + \gamma_n P_{cd,n}(k) \end{cases} \tag{8}$$

To represent the aggregated TCL's virtual battery model, (8) is rewritten as:

$$\sum_{j=1}^{n} \frac{x_j(k+1)}{\gamma_j} = \sum_{j=1}^{n} \kappa_j \frac{x_j(k)}{\gamma_j} + \sum_{j=1}^{n} P_{cd,j}(k) \tag{9}$$

Here, $SOC(k)$ and $P(k)$ for aggregated TCLs' virtual battery are defined as:

$$SOC(k) = \sum_{j=1}^{n} \frac{x_j(k)}{\gamma_j} \tag{10a}$$

$$P(k) = \sum_{j=1}^{n} P_{cd,j}(k) \tag{10b}$$

Considering (8)-(10b), the aggregated TCL flexibility is approximately expressed as:

$$P_{\min} \le P(k) \le P_{\max} \tag{11a}$$

$$SOC(k+1) = \alpha SOC(k) + P(k) \tag{11b}$$

$$SOC_{\min} \le SOC(k+1) \le SOC_{\max} \tag{11c}$$

where

$$P_{\max} = \sum_{j=1}^{n} \left( P_{rated,j} - \frac{T_{out} - T_{set,j}}{COP_j \cdot R_j} \right) \tag{11d}$$

$$P_{\min} = -\sum_{j=1}^{n} \frac{T_{out} - T_{set,j}}{COP_j \cdot R_j} \tag{11e}$$

$$SOC_{\min} = -\sum_{j=1}^{n} \frac{\delta_j}{COP_j \cdot R_j \cdot \left(1 - \exp\left(-\frac{\Delta t}{R_j \cdot C_{a,j}}\right)\right)} \tag{11h}$$

$$SOC_{\max} = \sum_{j=1}^{n} \frac{\delta_j}{COP_j \cdot R_j \cdot \left(1 - \exp\left(-\frac{\Delta t}{R_j \cdot C_{a,j}}\right)\right)} \tag{11f}$$

$$\alpha = \frac{1}{n} \sum_{j=1}^{n} \exp\left(-\frac{\Delta t}{R_j \cdot C_{a,j}}\right) \tag{11g}$$

It is noted that $\kappa$ in (9) varies for different TCLs' virtual batteries, which makes it difficult to aggregate a virtual battery population. For simplicity, $\alpha$ in (11b) is the average $\kappa$ for all virtual batteries as described in (11g). Hence, a TCL population's aggregated flexibility managed by an aggregator is built as a virtual battery model stated in (11a)-(11c). The aggregator will access virtual battery parameters using the TCL's probability distribution derived from the total TCL power [5]. Accordingly, TCLs will be scheduled like conventional batteries.

### *B. De-Aggregation of TCLs at the Lower Stage*

When aggregators receive trading results from the upper-stage, they decomposed the desired power into control signals to regulate TCLs in the de-aggregation process. To preserve TCL information privacy (i.e., TCL parameters, including $C_a$, $R$, $\delta$, $COP$) and customer preferences (i.e., $T_{\text{set}}$), the aggregator organizes a virtual market, which is a market-based control mechanism to drive self-interested TCLs to follow the desired power. Price signals are applied as control information to guide TCLs' performances; although, economic behavior is

not a consideration at this stage. Specifically, TCLs as sellers submit bids for power and price according to their operating status. It is assumed that there is only one virtual buyer for the desired power which pay the market clearing price. The aggregator collects bids, clears the virtual market, and sends the market clearing price to TCLs. TCLs will respond accordingly by submitting revised bids. The virtual market mechanism is portrayed as follows.

As charging/discharging schedules of virtual batteries are calculated at the upper stage, the desired TCL power is stated as:

$$P_{desired}(k) = \sum_{j=1}^{n} P_{baseline,j} + P(k) \tag{12}$$

Accordingly, the power adjustment (i.e., virtual buyer's purchased power) is represented as:

$$\Delta P(k) = P_{desired}(k) - P_{actual}(k) \tag{13}$$

If $\Delta P(k)>0$, certain TCLs will be turned on to be charged (charging market) and others will be turned off to be discharged (discharging market), which allow TCLs to submit bids strategically and in accordance with their operating states. Each TCL is installed with a smart controller for monitoring its operating status, calculate the related parameters, and communicate with the aggregator. Also, TCL bids are determined by their operating states. The market-based TCL control process is described as follow.

*Step 1:* TCLs decide if they are eligible to partake in a virtual market. In the charging market, only TCLs in off state can submit bids to charge their virtual batteries. Other TCLs in on state will participate in the discharging market to discharge their virtual batteries.

*Step 2:* When eligible TCLs submit bids, the clearing price will be determined. There are two main components to be considered in the bid price.

*1) TCL Compressor Wear-and-Tear:* Excessive switching can increase the stress on TCL compressors and potentially shorten their operating lives [28]. To relieve the mechanical stress, $\rho_1$ determined by the location of TCL internal temperature is developed. In the charging market, $\rho_1$ is calculated as:

$$\rho_1 = \frac{T_{\max} - T_{in}(k)}{T_{\max} - T_{\min}} \tag{14a}$$

indicating that the TCL with an internal temperature closer to $T_{max}$ has a lower price and is easier to be scheduled in the charging market, which reduces switching cycles. Similarly, $\rho_1$ in the discharging market is given as:

$$\rho_1 = \frac{T_{in}(k) - T_{\min}}{T_{\max} - T_{\min}}. \tag{14b}$$

*2) Fairness in Regulation:* Some TCLs are turned off/on excessively, while others are rarely manipulated during the regulation process. This unfair regulation process can irritate certain end users. Thus, $\rho_2$ is proposed to influence the fairness in bid price:

$$\rho_2 = \frac{N_r}{N_t} \tag{15}$$

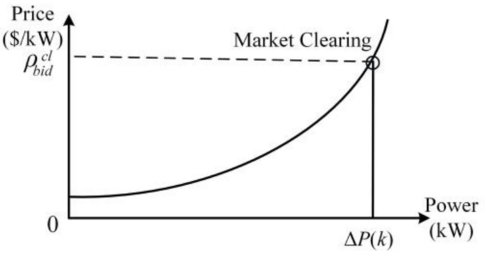


Fig. 2. Market clearing in TCL de-aggregation process.

Higher numbers of TCL switching will result in a larger $\rho_2$, indicating that the TCL is more difficult to be scheduled. Here, $\rho_{\text{bid}}$ consists of two price components which are stated as

$$\rho_{bid} = \omega_1 \cdot \rho_1 + \omega_2 \cdot \rho_2 \tag{16}$$

$$\omega_1 + \omega_2 = 1 \tag{17}$$

Each customer can decide $\omega_1$ and $\omega_2$ according to its preferences. For simplicity, $\omega_1$ and $\omega_2$ are assumed to be 1/2 in this paper. In addition, as TCL power can only be changed from $P_{\text{rated}}$ to 0 or 0 to $P_{\text{rated}}$, $P_{\text{rated}}$ is used as bid power.

*Step 3:* Aggregators collect TCL bids, sort out prices in ascending order and clear the market based on virtual buyer's required power, $\Delta P(k)$, as depicted in Fig. 2. As scheduling results are obtained from the upper stage using the aggregated TCLs' virtual battery model, there is always a market clearing price between the lowest and the highest TCL bid prices as depicted in Fig. 2.

The aggregator sends the corresponding market clearing price ($\rho_{bid}^{cl}$) to participating TCLs for comparison with respective bid prices. If $\rho_{bid}^{cl}$ is higher, TCL will switch its state; otherwise, TCL will keep its state. In this regard, TCLs will not provide their parameters to aggregators in order to protect end-user's information privacy.

## IV. Transactive Energy Market Operation with Aggregated TCL Flexibility

It is assumed that distributed generators and loads connected to a power network node are also managed by TCL aggregators. Accordingly, distributed generators, virtual batteries and inelastic loads are regulated by an aggregator to take part in the power system operation. To preserve the information privacy, aggregators at the upper stage coordinate a peer-to-peer energy trading in power systems. The information transacted among aggregators includes electricity price and demand. However, distributed resource parameters managed by aggregators will not be communicated. The detailed scheduling strategy is described as follows.

The primal objective is to minimize the total operation cost of $N_{\text{agg}}$ aggregators, which is formulated as:

$$L = \min \sum_{k=1}^{N_k} \sum_{i=1}^{N_{agg}} \begin{pmatrix} C_g\left(P_{G,i}(k)\right) + \rho_i(k) \cdot P_{pur,iSO}(k) \\ + \sum_{v=1}^{N_{agg}} d_{iv} \cdot \left(P_{pur,iv}(k)\right)^2 \end{pmatrix} \tag{18}$$

where the first term is the generator cost expressed as $C_{\text{g}}(x) = ax^2 + bx + c$. The second term is the aggregator's cost for purchasing power from system operator (SO). The aggregator

which purchases power from other aggregators also pays for power losses in the trading process. Thus, the third term is the delivery cost when aggregators purchase power from other aggregators in which the quadratic power loss is taken into account [30].

The primal constraints are given as:

$$P_{G,i}(k) + P_{pur,iSO}(k) + \sum_{v=1}^{N_{agg}} P_{pur,iv}(k) - P_{sel,i}(k) - P_{battery,i}(k) - P_{load,i}(k) = 0,\ 1 \le i \le N_{agg} \quad (19a)$$

$$0 \le P_{G,i}(k) \le P_{G,\max},\ 1 \le i \le N_{agg} \quad (19b)$$

$$0 \le P_{pur,iv} \le P_{pur,\max}, P_{pur,ii} = 0,\ 1 \le i \le N_{agg}, 1 \le v \le N_{agg} \quad (19c)$$

$$P_{sel,i}(k) \ge 0, 1 \le i \le N_{agg} \quad (19d)$$

$$P_{sel,i}(k) = \sum_{v=1}^{N_{agg}} P_{pur,vi}(k), 1 \le i \le N_{agg} \quad (19e)$$

$$P_{pur,iSO}(k) \ge 0, 1 \le i \le N_{agg} \quad (19f)$$

Constrains of virtual battery model (2a)-(2c) (19g)

where (19a) is the power balance of AGG $i(1 \le i \le N_{\text{agg}})$. Equation (19b) is the generator $i$ power constraint $(1 \le i \le N_{\text{agg}})$. Equation (19c)-(19e) are aggregators' transacted power constraints. Equation (19f) is the purchased power constraint of the aggregator from SO. Equation (19g) is the set of power constraints of aggregated TCLs provided in Section III.

Lagrangian relaxation is utilized here to address peer-to-peer transactions that would protect each aggregator's information privacy. The primal problem is decoupled into aggregator subproblems. Each aggregator will transact with other aggregators using trading signals to achieve optimal operations. The Lagrangian function is stated as:

$$F = \min \sum_{k=1}^{N_k} \sum_{i=1}^{N_{agg}} \begin{pmatrix} C_g\left(P_{G,i}(k)\right) + \rho_i(k) \cdot P_{pur,iSO}(k) \\ + \sum_{v=1}^{N_{agg}} d_{iv} \cdot \left(P_{pur,iv}(k)\right)^2 + \lambda_i(k)\left(P_{pur,1i}(k)\right. \\ \left. + P_{pur,2i}(k) + \cdots + P_{pur,N_{agg}i}(k) - P_{sel,i}(k)\right) \end{pmatrix} \quad (20)$$

Here, (20) will be decomposed into aggregator subproblems in which the optimization model of AGG $i$ for peer-to-peer transactions is expressed in (21). Each aggregator solves its cost minimization problem expressed as (21). However, $N_{\text{agg}}$ aggregator solutions cannot satisfy the power balance constraint in the primal problem (19e). Accordingly, $\lambda_i$ and $P_{pur,i1}$, $P_{pur,i2}, \ldots, P_{pur,iN_{agg}}$ are exchanged between AGG $i$ and other aggregators. The subgradient method is employed to update the multipliers.

$$F_i = \min \sum_{k=1}^{N_k} \begin{pmatrix} C_g\left(P_{G,i}(k)\right) + \rho_i(k) \cdot P_{pur,iSO}(k) \\ + \sum_{v=1}^{N_{agg}} d_{iv} \cdot \left(P_{pur,iv}(k)\right)^2 + \lambda_1(k) \cdot P_{pur,i1}(k) \\ + \lambda_2(k) \cdot P_{pur,i2}(k) + \cdots + \lambda_{N_{agg}}(k) \cdot P_{pur,iN_{agg}}(k) \\ - \lambda_i(k) \cdot P_{sel,i}(k) \end{pmatrix} \quad (21)$$

s.t. (19a) - (19d) and (19f) - (19g).

$$\lambda_i(k)[m+1] = \lambda_i(k)[m]$$

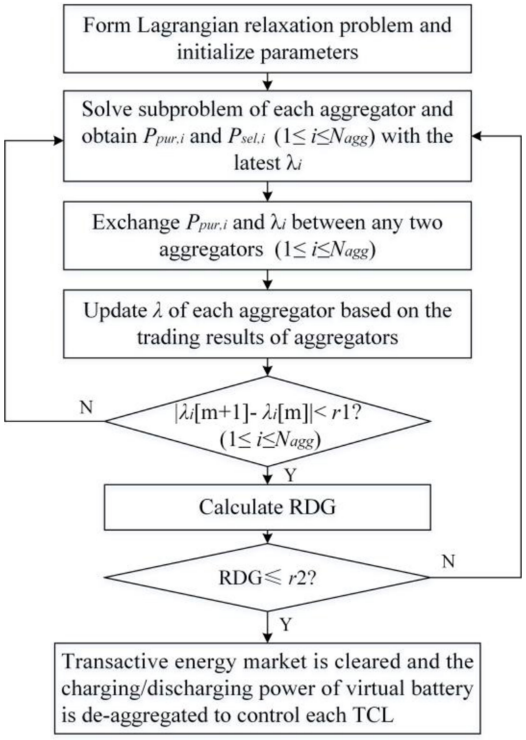


Fig. 3. Flowchart of aggregators' trading process.

$$+ \frac{1}{h \cdot m + l}\left(\sum_{v=1}^{N_{agg}} P_{pur,vi}(k)[m] - P_{sel,i}(k)[m]\right) \quad (22)$$

In (22), the updated $\lambda_i$ reflects the AGG *i's* supply and demand relation in the market. When demand is less than supply (i.e., $\sum_{v=1}^{N_{agg}} P_{pur,vi}(k) < P_{sel,i}(k)$), $\lambda_i$ will be lowered. Otherwise, $\lambda_i$ will become larger. Thus, $\lambda_i$ is treated as the AGG *i's* biding price and the final $\lambda_i$ is the AGG *i*'s market clearing price. Moreover, $\lambda_1(k)P_{pur,i1}(k) + \lambda_2(k)P_{pur,i2}(k) + \cdots + \lambda_{N_{agg}}(k)P_{pur,iN_{agg}}(k)$ in (21) is the AGG *i's* cost when it purchases power from other aggregators. $\lambda_i(k)P_{sel,i}(k)$ is the AGG *i's* income when it sells power. The difference between the two is the AGG *i's* cost for energy transaction, which reflects AGG *i's* market cost and revenue. Such a peer-to-peer market mechanism which balances supply and demand using electricity price as a key parameter is presented as the transactive energy market [31].

The flowchart of aggregators' trading process is given in Fig. 3, and the aggregators' transactive process is described as follows.

(1) Form the Lagrangian relaxation problem (20) and initialize parameters, including $\lambda_i(1 \le i \le N_{\text{agg}})$, the power grid structure, AGG contract prices, generator cost curve, load curve, and virtual battery model;

(2) Solve each aggregator's subproblem (21) with the latest $\lambda_i(1 \le i \le N_{\text{agg}})$. Then each aggregator $i$ gets its $P_{pur,iv}$ and $P_{sel,i}(1 \le v \le N_{\text{agg}},\ v \ne i)$ according to other aggregators' prices. Repeat Step (2), and calculate $P_{pur}$ and $P_{sel}$ for each aggregator;

(3) It is assumed that aggregators are able to communicate with each other by a local communication network. Exchange

TABLE I
TCL PARAMETER RANGES OF AGGREGATORS

| Parameters | AGG1 | AGG2 | AGG3 |
|---|---|---|---|
| $T_{set}$ | 15-25°C | 20-25 °C | 20-22.5 °C |
| $\delta$ | 0.25-1 °C | 0.25-0.35 °C | 0.3-0.5 °C |
| $R$ | 1.5-2.5 °C/kW | 1.8-2.2 °C/kW | 2 °C/kW |
| $C_a$ | 1.5-2.5kWh/ °C | 1.8-2.2 kWh/ °C | 2 kWh/ °C |
| $P_{rated}$ | 10-18kW | 4.5-7 kW | 6-14 kW |
| $COP$ | 2.5 | 2.5 | 2.5 |

TABLE II
COEFFICIENTS OF GENERATOR COST FUNCTION

| Aggregator | $a$ (\$/kW$^2$) | $b$ (\$/kW) | $c$ (\$) |
|---|---|---|---|
| AGG1 | 1.22e (-6) | 0.04 | 0.35 |
| AGG2 | 1.12e (-6) | 0.02 | 0.25 |
| AGG3 | 8.65e (-7) | 0.03 | 0.40 |

TABLE III
PARAMETERS OF VIRTUAL BATTERIES

| Aggregator | $P_{min}$ (MW) | $P_{max}$ (MW) | $SOC_{min}$ (MW) | $SOC_{max}$ (MW) | $\alpha$ |
|---|---|---|---|---|---|
| AGG1 | -3.24 | 10.76 | -6.15 | 6.15 | 0.98 |
| AGG2 | -2.71 | 3.02 | -2.89 | 2.89 | 0.98 |
| AGG3 | -2.94 | 6.93 | -3.86 | 3.86 | 0.98 |

$P_{pur}$ and $\lambda$ between any two aggregators. Each aggregator gets the access to other aggregators' trading results and prices;

(4) Update each aggregator's $\lambda$ using the trading results in terms of (22). If each aggregator's $\lambda$ does not change much in two consecutive iterations (i.e., $|\lambda[m+1]-\lambda[m]| \leq r1$, with r1 representing the termination threshold), $\lambda$ is a feasible solution and go to Step (5); otherwise, go to Step (2);

(5) Calculate the primal objective value $L$ in (18) and $F$ in (20) according to each aggregator's latest trading results. The upper bound of the optimal value $L^*$ of (18) is given by $L$ and the lower bound is provided by $F$. Analyze the relative duality gap (RDG) (see (23)). Check whether RDG $\leq$ r2, where r2 is the termination threshold. If satisfied, the trading results in the transactive market are the same as the primal optimization problem described in (19a)-(19g); go to Step (6). Otherwise, more trading iterations are required; go back to Step (2).

$$RDG = \left|\frac{L-F}{F}\right| \tag{23}$$

(6) Transactive energy market is cleared and each aggregator's trading is determined. Accordingly, each virtual battery's charging/discharging power regulated by aggregators is also decided, which is sent to the lower stage for de-aggregation to control individual TCLs.

Hence, TCLs are regulated by virtual market signals at the lower stage and scheduled in a transactive energy market at the upper stage. In this way, the TCL information will not be leaked to aggregators and aggregators will not expose the information to their peers.

## V. CASE STUDIES

We assume there are three aggregators represented as AGG1-AGG3. TCL parameters of each aggregator are shown in Table I. The number of TCLs in each AGG is 1,000. The ambient temperature is 36°C. The time slots at upper and lower stages are 5 minutes and 1 minute, respectively. Generation cost function coefficients for AGG1-AGG3 are shown in Table II. The generator capacities for AGG1-AGG3 are 7.5MW, 10MW, and 12MW, respectively. Loads are scaled [32]; r1 and r2 are 0.05; $d_{12}$, $d_{13}$ and $d_{23}$ (representing actual distances) are $4\times10^{-4}$ \$/MW$^2$, $1.4\times10^{-3}$ \$/MW$^2$ and $1.8\times10^{-3}$ \$/MW$^2$.

To validate the proposed methods and highlight our main contributions, case studies are structured as follows. The simulations in Sections V-A and V-B are employed to analyze aggregators' trading behaviors at the upper stage and the control performance of TCLs at the lower stage, respectively. The scheduling of TCLs at two stages are coordinated to regulate TCLs. Section V-C compares virtual and conventional battery models based on the virtual battery's scheduling results provided in Section V-A.

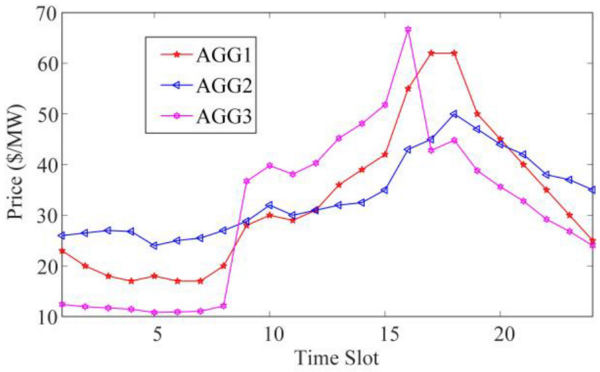


Fig. 4. SO's contract prices of AGG1 - AGG3.

### A. Aggregators' Transactive Trading Results at the Upper Stage

Using our proposed model, virtual battery parameters are calculated and shown in Table III. The contract price of AGG1-AGG3 is previously determined by SO and depicted in Fig. 4 [33]. Aggregators with flexible TCLs participate in the proposed peer-to-peer trading. Each aggregator makes trading decisions based on other aggregators' prices, SO contract prices and local generation costs, without leaking any proprietary information. Simulation results are presented as follows. The behaviors of entities (including aggregators, generators, and virtual battery) and prices (including SO contract prices, generators' marginal costs and aggregators' trading prices) are all analyzed to show the operating mechanism of the proposed peer-to-peer trading. Two Cases with and without peer-to-peer trading are also compared to show that the peer-to-peer trading can reduce the operation cost in the power system.

(1) *Analyses of power provided by SO and local generation:* Figs. 5-6 show the power purchased from SO and generators' power and marginal costs, respectively. Here, any purchases

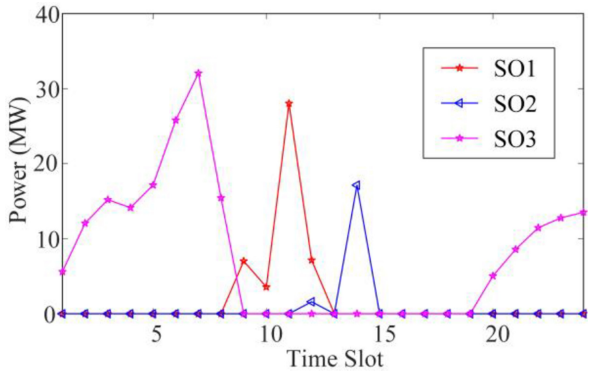


Fig. 5. Power purchased by AGG1-AGG3 from SO.

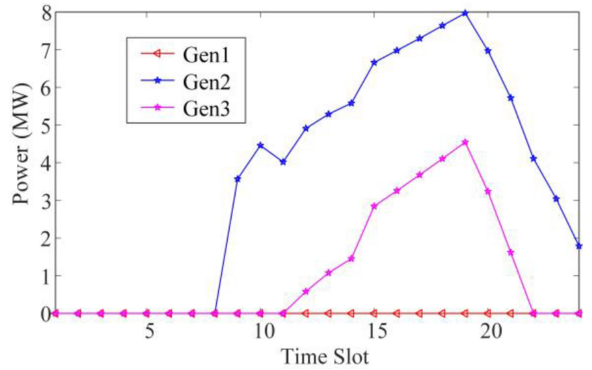


Fig. 6. Generator power of AGG1-AGG3.

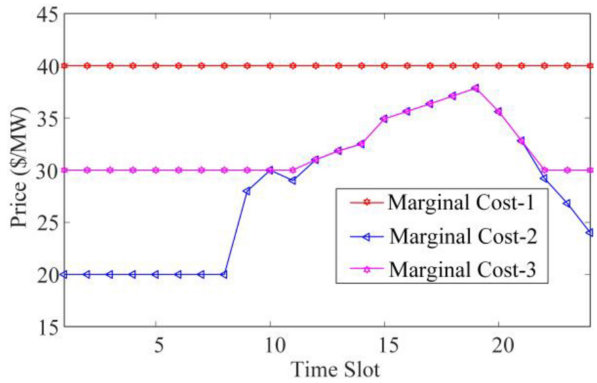


Fig. 7. Generator marginal cost of AGG1-AGG3.

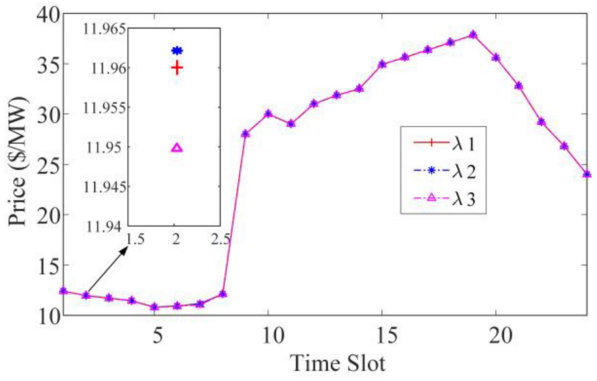


Fig. 8. Transactive trading price of AGG1-AGG3.

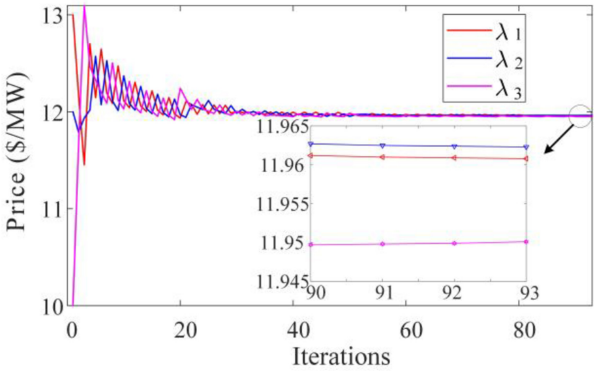


Fig. 9. Transactive trading price convergence in time slot 2.

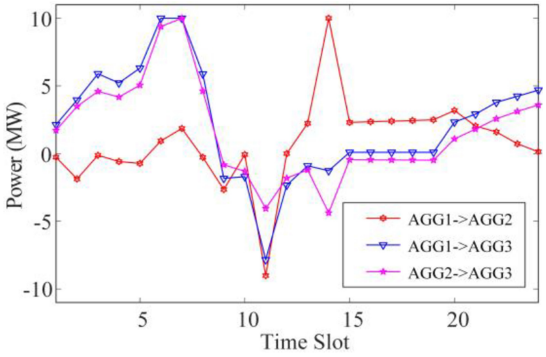


Fig. 10. Transactive trading power between AGG1-AGG3.

depend on the SO's price and the generator marginal cost. Considering the results in Figs. 5-7, AGG3 purchases more power from SO at time slots 1-8, when SO's price is lower than that of AGG1-AGG2 and the generator marginal cost of AGG1-AGG3. At this time, generators as more expensive resources will not be dispatched. When the SO's price is higher (e.g., time slots 15-19), generators of AGG2 and AGG3 with lower marginal costs, as compared with those of AGG1, are dispatched.

(2) *Analyses of aggregators' trading prices:* Fig. 8 shows transactive trading prices ($\lambda_1$, $\lambda_2$ and $\lambda_3$) of AGG1-AGG3 which have overlapped due to small differences of $\lambda_1$, $\lambda_2$ and $\lambda_3$. It is clear that the trends in aggregator trading prices are consistent with the SO's price for AGG3 at time slots 1-8, when the corresponding SO's price is the lowest as compared to other SO prices and generator marginal costs. When any aggregators' generator marginal costs are lower than the SO's price, the trading price trends are consistent with generator marginal costs in AGG1 and AGG2 at time slots 15-19. In this example, aggregators' trading prices reflect those of cheapest dispatched resources (SO or generators).

Take $\lambda_1$ - $\lambda_3$ at time slot 2 to analyze the transactive trading among AGG1-AGG3. The convergence of $\lambda_1$ - $\lambda_3$ at time slot 2 is depicted in Fig. 9. The corresponding trading power is shown in Fig. 10. Here, $\lambda_3 = 11.9501$ is the lowest compared with $\lambda_1 = 11.9608$ and $\lambda_2 = 11.9623$, which means the cheapest resource is scheduled by AGG3. Thus, both AGG1 and AGG2 purchase power from AGG3. Moreover, purchasing

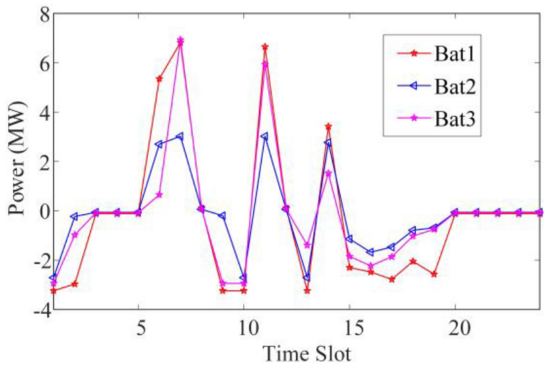


Fig. 11. Virtual battery charging/discharging power of AGG1-AGG3.

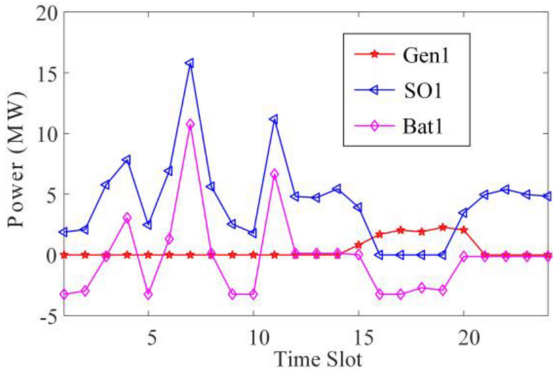


Fig. 12. AGG1 operation in Case 2.

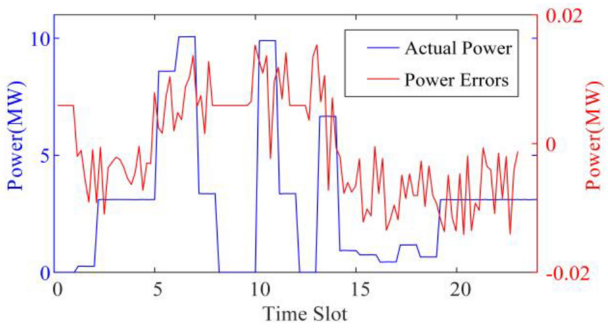


Fig. 13. Actual power and power errors of TCLs in AGG1.

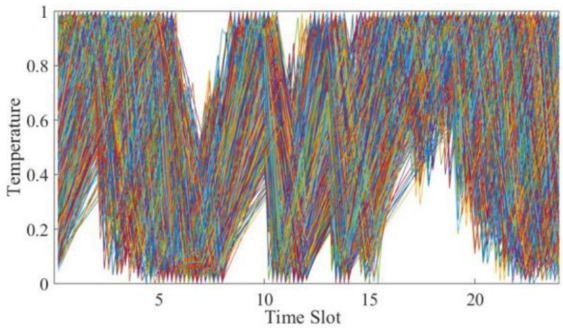


Fig. 14. TCL internal temperature profiles of AGG1.

aggregators also pay for transmission losses. So, AGG2 also buys power from AGG1 to reflect a shorter electrical distance. The differences among $\lambda 1$, $\lambda 2$ and $\lambda 3$ describe the trading power direction among AGG1-AGG3. Aggregators will operate economically by adopting the trading price $\lambda$ in the peer-to-peer transaction process.

(3) *Analysis of virtual battery:* The virtual batteries' operations are shown in Fig. 11 in which virtual batteries in AGG1-AGG3 have similar operating behaviors. Virtual batteries are either charging or discharging when transactive trading prices in Fig. 8 are lower (e.g., at time slots 5-7) or higher (e.g., at time slots 15-19), respectively. This Case demonstrates that virtual batteries' operating behaviors are determined by the trend in aggregator trading prices.

(4) *Comparison of aggregator's behaviors with and without peer-to-peer transactive trading:* Two Cases are compared to show the effectiveness of the proposed peer-to-peer transactive trading. Aggregators with flexible TCLs participate in the proposed peer-to-peer trading in Case 1. Such aggregators do not participate in the proposed transactive energy market and only purchase electricity from SO in Case 2 (i.e., in Case 2, there are only transactions between SO and aggregators). The dispatched power of generators and SO are determined by generator marginal costs and SO prices. The operating behaviors of AGG1 in Case 2 are presented in Fig. 12. If the SO's price is lower than generator marginal costs, aggregators will purchase power from SO and virtual batteries are charged (e.g., time slot 4 for AGG1 in Fig. 12). If the SO's price is higher than generator marginal prices, aggregators will generate power and virtual batteries are discharged (e.g., time slots 17-18 for AGG1). The total costs in two Cases are \$8,151.8 and \$9,486.1, respectively. In Case 2, aggregators cannot trade any cheaper power with other aggregators, which increases the operation cost as compared to that in Case 1.

### *B. Control Performances of TCLs at the Lower Stage*

The scheduled power of aggregated TCLs (i.e., charging/discharging power of virtual battery) is determined when the transactive market is cleared at the upper stage. Then the aggregator will de-aggregate the scheduled power to control each TCL in terms of the proposed method in Section III-B.

Take AGG1 as an example to validate the proposed virtual battery model and the control method of TCLs. The TCL's actual power and errors (representing differences between the desired and the actual TCL power) are shown in Fig. 13, and the corresponding internal temperature profiles are given in Fig. 14. Different colors in Fig. 14 represent TCLs' profiles for respective control signals [28], [29]. TCLs' diverse internal temperatures are normalized in Fig. 14. In Fig. 13, power errors are very small, which means TCLs can closely track the virtual battery's scheduled power that is determined at the upper stage. In Fig. 14, TCLs' internal temperatures are limited within [0, 1] for satisfying end users' comfort requirements. The outcome demonstrates that virtual batteries accurately describe the TCLs' aggregated flexibility as TCLs are effectively controlled by the proposed method.

When TCLs are regulated to follow the desired power, it is imperative to relieve the switching's mechanical stress as TCL's internal temperature is considered for implementing

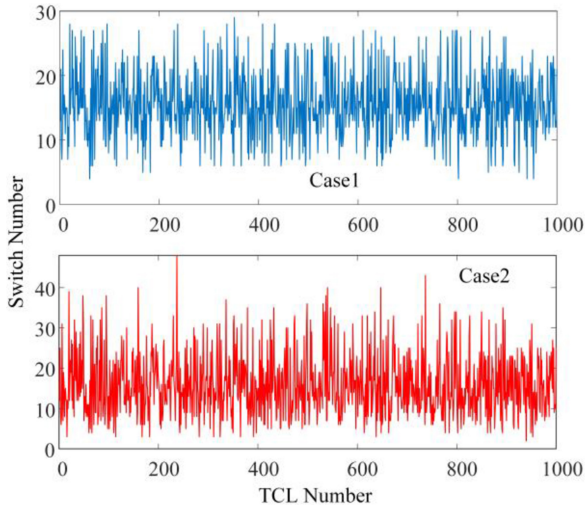


Fig. 15. Number of TCL switching in Cases 1 and 2.

TABLE IV
$P_{\min}$ AND $P_{\max}$ OF VIRTUAL BATTERY FOR DIFFERENT EXTERNAL TEMPERATURES

| $T_{out}$ (°C) | 36 | 37.5 | 38 | 37 |
|---|---|---|---|---|
| $P_{\min}$ (MW) | -3.24 | -3.58 | -3.66 | -3.44 |
| $P_{\max}$(MW) | 10.76 | 10.40 | 10.37 | 10.64 |

ascending/descending orders in centralized control [7], [28]. The switching's mechanical stress is also relieved in the proposed transactive control when TCL's internal temperature is considered as bid. Two Cases are compared to show the other merits of the proposed transactive control at the lower stage. In Case 1, the TCL bid is composed of TCL's internal temperature and regulation fairness (i.e., $\omega_1 = 1/2$, $\omega_2 = 1/2$). In Case 2, only TCL's internal temperature is considered in TCL bid (i.e., $\omega_1 = 1$, $\omega_2 = 0$). The numbers of TCL switching in Cases 1 and 2 are provided in Fig. 15. The corresponding variances of the number of TCL switching in the two Cases are 23.34 and 55.15, respectively. It is clear that the proposed method will effectively avoid unfair regulations where some TCLs are turned off/on excessively.

### C. Comparison of Conventional and Virtual Batteries

Although the virtual battery shares the same models with conventional lithium-ion battery, there are differences between the two models as presented below.

(1) *Virtual battery is sensitive to external temperatures:* External temperatures affect virtual batteries' operating behaviors. Generally, external temperature would change continuously, and we assume external temperatures remain fixed in half-hour intervals. The $P_{\min}$ and $P_{\max}$ in AGG1's virtual battery for different external temperatures are calculated in Table IV. The conventional battery is required to work within a certain range of ambient temperature. Even though, a conventional battery's operating behavior cannot change as significantly as that of a virtual battery when external temperature changes within a normal range.

TABLE V
PARAMETERS OF LITHIUM-ION BATTERY

| Parameter | $P^d$ | $P^c$ | $\eta^c$ | $\eta^d$ |
|---|---|---|---|---|
| Value | 5/MW | 5/MW | 0.95 | 0.95 |
| Parameter | $o$ | $soc_{min}$ | $soc_{max}$ | $soc_0$ |
| Value | 9/MWh | 0 | 1 | 0.5 |

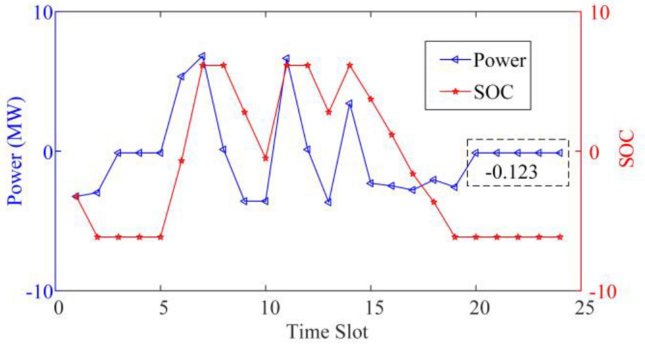


Fig. 16. Operating behavior of virtual battery in AGG1.

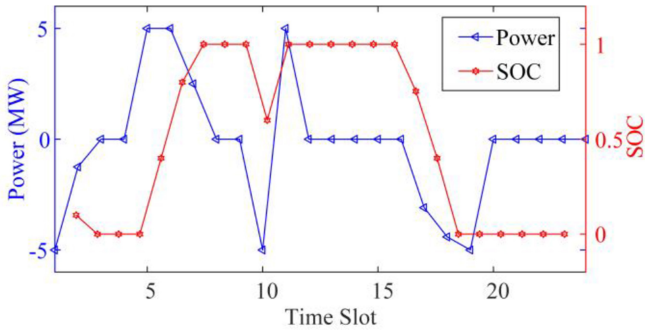


Fig. 17. Operating behavior of lithium-ion battery.

(2) *Virtual battery shows an infinite capacity in some Cases:* The virtual battery's operating behavior in AGG1 is shown in Fig. 16, where the aggregators' total cost is \$8,151.8. To compare virtual and conventional batteries in terms of operating behaviors, a lithium-ion battery with parameters stated in Table V is scheduled in the peer-to-peer transactive trading with a similar total cost of \$8,131.8. In Fig. 16, SOC is fixed even though the virtual battery is slightly charged/discharged in certain time slots (e.g., hours 20-24) with an infinite capacity which will never be fully charged/discharged. By contrast, SOC can only stay fixed when the lithium-ion battery's charging/discharging power is 0 (e.g., time slot 20-24 hours in Fig. 17). The corresponding explanation is given as follows.

For a virtual battery, $SOC(k+1)$ is equal to $SOC(k)$ when $P(k)$ is given as:

$$P(k) = (1-\alpha) \cdot SOC(k) \tag{24}$$

In (24), $P(k)$ will not be 0 as $SOC(k)$ is not within ($0< \alpha <1$). This means that the energy storage level of a virtual battery does not change even though it is charging/discharging. In this case, we assume the TCL's virtual battery has an infinite capacity which cannot be fully charged/discharged. A TCL will consume a certain amount of power, which will be adjusted with temperature, in order to maintain a fixed

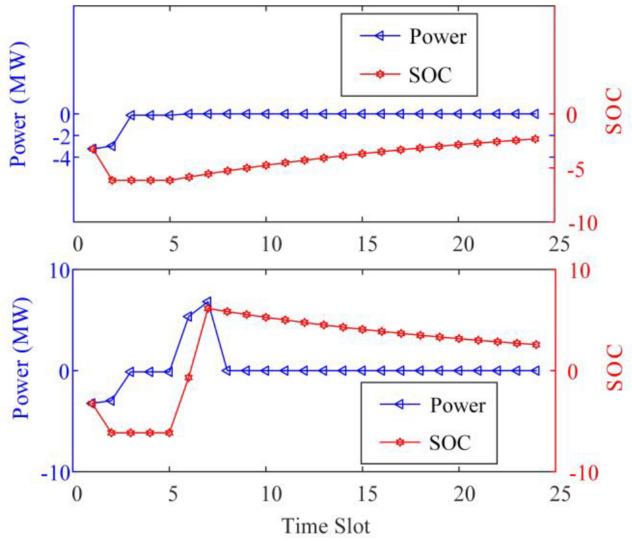


Fig. 18. Operating behavior of virtual battery.

internal temperature. $P(k)$ is defined as the difference between the actual power and baseline power of TCLs according to (4a) and (10b). When the internal temperature is kept at a point that is different from $T_{\text{set}}$, the TCL's actual power is always different from the baseline power. In other words, a virtual battery would need to absorb/release some power to maintain its energy storage levels (i.e., $SOC(k) \neq 0$). Thus, a virtual battery possesses an unlimited capacity when $P(k)$ is equal to the power difference corresponding to TCL's internal temperatures at $T^*$ and $T_{\text{set}}$ ($T^* \neq T_{\text{set}}$), respectively. At this time, the virtual battery's energy storage level is fixed at $SOC(k)$ and the corresponding TCL internal temperature is $T^*$. By contrast, a conventional battery's energy storage level will change when charging/discharging power is not 0. This means a conventional battery has a limited capacity which can be fully charged/discharged.

(3) *Virtual battery has an automatic restoration capability:* The charging/discharging power is set at 0 between time slots 6 and 24. The corresponding relationship between $P(k)$ and $SOC(k)$ is simulated in the upper Fig. 18, where the SOC gradually approaches 0. Similarly, the relationship between $P(k)$ and $SOC(k)$ is shown in the lower Fig. 18, when $P(k)$ is 0 beyond the time slot 7 when $SOC(k)$ also approaches 0. The corresponding explanation is given as follows.

$SOC(k+1)$ changes according to $SOC(k)$ and the absolute value of $SOC(k+1)$ will be less than that of $SOC(k)$ when $P(k)$ is 0 ($0< \alpha <1$) in (11b). If $SOC(k)>0$, $SOC(k+1)$ is smaller than $SOC(k)$, which means the energy storage level is reduced. If $SOC(k) < 0$, $SOC(k+1)$ is larger than $SOC(k)$, which means the energy storage level is increased. Hence, $SOC(k+1)$ tends to approach 0 (its original state) when $P(k)$ is 0. This phenomenon is related to the self-dissipation power of a virtual battery. When $SOC(k)>0$, a virtual battery will self-dissipate power and $P(k)$ is too small to maintain the current energy storage level, which will result in a lower SOC. When $SOC(k)<0$, the self-dissipated power of a virtual battery is smaller than 0 and $P(k)$ is too large to maintain the current energy storage level, which will result in a higher SOC. However, for a conventional battery, $SOC(k+1)$ is equal to $SOC(k)$ when $P(k)$ is 0. This means a conventional battery's energy storage level remains constant when it is not deployed.

## VI. Conclusion

A hierarchical coordination mechanism is proposed to manage the TCL flexibility in a distributed fashion. TCLs are regulated by the transactive control and TCL flexibilities are aggregated using a virtual battery model at the lower stage. Compared with a conventional battery, the proposed virtual battery is more sensitive to external temperatures when the temperature is changing within a normal range, offers an infinite capacity in some cases, and has an automatic restoration capability. A transactive energy market enables aggregators with TCL flexibility to trade with each other for minimizing the cost of power system at the upper stage. The effectiveness of the proposed methods is validated by several case studies. Our future work will focus on enhancing the resilience of power systems via transactive energy markets by utilizing distributed resources, including TCLs, electric vehicles and conventional batteries.

## References

[1] H. Wu, M. Shahidehpour, A. Alabdulwahab, and A. Abusorrah, "Thermal generation flexibility with ramping costs and hourly demand response in stochastic security-constrained scheduling of variable energy sources," *IEEE Trans. Power Syst.*, vol. 30, no. 6, pp. 2955–2964, Nov. 2015.

[2] I. A. Sajjad, G. Chicco, and R. Napoli, "Definitions of demand flexibility for aggregate residential loads," *IEEE Trans. Smart Grid*, vol. 7, no. 6, pp. 2633–2643, Nov. 2016.

[3] Y.-J. Kim, L. K. Norford, and J. L. Kirtley, "Modeling and analysis of a variable speed heat pump for frequency regulation through direct load control," *IEEE Trans. Power Syst.*, vol. 30, no. 1, pp. 397–408, Jan. 2015.

[4] N. Lu and Y. Zhang, "Design considerations of a centralized load controller using thermostatically controlled appliances for continuous regulation reserves," *IEEE Trans. Smart Grid*, vol. 4, no. 2, pp. 914–921, Jun. 2013.

[5] M. Song, C. Gao, M. Shahidehpour, Z. Li, S. Lu, and G. Lin, "Multi-time-scale modeling and parameter estimation of TCLs for smoothing out wind power generation variability," *IEEE Trans. Sustain. Energy*, vol. 10, no. 1, pp. 105–118, Jan. 2019.

[6] J. T. Hughes, A. D. Domínguez-García, and K. Poolla, "Identification of virtual battery models for flexible loads," *IEEE Trans. Power Syst.*, vol. 31, no. 6, pp. 4660–4669, Nov. 2016.

[7] H. Hao, B. M. Sanandaji, K. Poolla, and T. L. Vincent, "Aggregate flexibility of thermostatically controlled loads," *IEEE Trans. Power Syst.*, vol. 30, no. 1, pp. 189–198, Jan. 2015.

[8] L. Zhao, W. Zhang, H. Hao, and K. Kalsi, "A geometric approach to aggregate flexibility modeling of thermostatically controlled loads," *IEEE Trans. Power Syst.*, vol. 32, no. 6, pp. 4721–4731, Nov. 2017.

[9] J. L. Mathieu, M. Kamgarpour, J. Lygeros, G. Andersson, and D. S. Callaway, "Arbitraging intraday wholesale energy market prices with aggregations of thermostatic loads," *IEEE Trans. Power Syst.*, vol. 30, no. 2, pp. 763–772, Mar. 2015.

[10] V. Trovato, S. H. Tindemans, and G. Strbac, "Leaky storage model for optimal multi-service allocation of thermostatic loads," *IET Gener. Transm. Distrib.*, vol. 10, no. 3, pp. 585–593, 2016.

[11] H. Hao, D. Wu, J. Lian, and T. Yang, "Optimal coordination of building loads and energy storage for power grid and end user services," *IEEE Trans. Smart Grid*, vol. 9, no. 5, pp. 4335–4345, Sep. 2018.

[12] N. S. Raman and P. Barooah, "On the round-trip efficiency of an HVAC-based virtual battery," *IEEE Trans. Smart Grid*, to be published, doi: 10.1109/TSG.2019.2923588.

[13] J. Hu *et al.*, "Load following of multiple heterogeneous TCL aggregators by centralized control," *IEEE Trans. Power Syst.*, vol. 32, no. 4, pp. 3157–3167, Jul. 2017.

[14] A. Radaideh, U. Vaidya, and V. Ajjarapu, "Sequential set-point control for heterogeneous thermostatically controlled loads through an extended Markov chain abstraction," *IEEE Trans. Smart Grid*, vol. 10, no. 1, pp. 116–127, Jan. 2019.
[15] A. Hussain, V.-H. Bui, and H.-M. Kim, "A resilient and privacy-preserving energy management strategy for networked microgrids," *IEEE Trans. Smart Grid*, vol. 9, no. 3, pp. 2127–2139, May 2018.
[16] J. Wu and X. Guan, "Coordinated multi-microgrids optimal control algorithm for smart distribution management system," *IEEE Trans. Smart Grid*, vol. 4, no. 4, pp. 2174–2181, Dec. 2013.
[17] F. Rahimi and A. Ipakchi, "Using a transactive energy framework: Providing grid services from smart buildings," *IEEE Electrific. Mag.*, vol. 4, no. 4, pp. 23–29, Dec. 2016.
[18] Z. Liu, Q. Wu, M. Shahidehpour, C. Li, S. Huang, and W. Wei, "Transactive real-time electric vehicle charging management for commercial buildings with PV on-site generation," *IEEE Trans. Smart Grid*, vol. 10, no. 5, pp. 4939–4950, Sep. 2019.
[19] Y. K. Renani, M. Ehsan, and M. Shahidehpour, "Optimal transactive market operations with distribution system operators," *IEEE Trans. Smart Grid*, vol. 9, no. 6, pp. 6692–6701, Nov. 2018.
[20] M. Case, D. Gregoratti, and J. Matamoros, "Distributed energy trading: The multiple-microgrid case," *IEEE Trans. Ind. Electron.*, vol. 62, no. 4, pp. 2551–2559, Apr. 2015.
[21] S. Somasundaram, R. G. Pratt, and B. A. Akyol, "Reference guide for a transaction-based building controls framework," Pacific Northwest Nat. Lab., Richland, WA, USA, Rep. PNNL-23302, Apr. 2014.
[22] S. Katipamula, D. P. Chassin, D. D. Hatley, R. G. Pratt, and D. J. Hammerstrom, "Transactive controls: Market-based gridwise controls for building systems," Pacific Northwest Nat. Lab., Richland, WA, NA, Rep. PNNL-17632, 2006.
[23] H. Hao, C. D. Corbin, K. Kalsi, and R. G. Pratt, "Transactive control of commercial buildings for demand response," *IEEE Trans. Power Syst.*, vol. 32, no. 1, pp. 774–783, Jan. 2017.
[24] S. Li, W. Zhang, J. Lian, and K. Kalsi, "Market-based coordination of thermostatically controlled loads—Part I: A mechanism design formulation," *IEEE Trans. Power Syst.*, vol. 31, no. 2, pp. 1170–1178, Mar. 2016.
[25] S. Li, W. Zhang, J. Lian, and K. Kalsi, "Market-based coordination of thermostatically controlled loads—Part II: Unknown parameters and case studies," *IEEE Trans. Power Syst.*, vol. 31, no. 2, pp. 1179–1187, Mar. 2016.
[26] T. Vidyamani and K. S. Swarup, "Analysis of active and transactive demand response strategies for smart residential buildings," in *Proc. 20th Nat. Power Syst. Conf.*, 2019, pp. 1–5.
[27] J. Ikäheimo, C. Evens, and S. Kärkkäinen, "DER aggregator business: The Finnish case," Tech. Res. Center Finland (VTT), Espoo, Finland, 2010.
[28] N. Lu, "An evaluation of the HVAC load potential for providing load balancing service," *IEEE Trans. Smart Grid*, vol. 3, no. 3, pp. 1263–1270, Sep. 2012.
[29] M. Song, C. Gao, M. Shahidehpour, Z. Li, and J. Yang, "State space modeling and control of aggregated TCLs for regulation services in power grids," *IEEE Trans. Smart Grid*, vol. 10, no. 4, pp. 4095–4106, Jul. 2019.
[30] Y. Wang, Z. Huang, M. Shahidehpour, L. L. Lai, Z. Wang, and Q. Zhu, "Reconfigurable distribution network for managing transactive energy in a multi-microgrid system," *IEEE Trans. Smart Grid*, to be published, doi: 10.1109/TSG.2019.2935565.
[31] Z. Liu, Q. Wu, S. Huang, and H. Zhao, "Transactive energy: A review of state of the art and implementation," in *Proc. IEEE Manchester PowerTech*, Manchester, U.K., Jun. 2017, pp. 1–6.
[32] M. Song, C. Gao, H. Yan, and J. Yang, "Thermal battery modeling of inverter air conditioning for demand response," *IEEE Trans. Smart Grid*, vol. 9, no. 6, pp. 5522–5534, Nov. 2018.
[33] L. Bai, J. Wang, C. Wang, C. Chen, and F. Li, "Distribution locational marginal pricing (DLMP) for congestion management and voltage support," *IEEE Trans. Power Syst.*, vol. 33, no. 4, pp. 4061–4073, Jul. 2018.

**Meng Song** received the B.S. degree from Southeast University, Nanjing, China, in 2012, the M.S. degree from the Harbin Institute of Technology, Harbin, China, in 2014, and the Ph.D. degree from Southeast University, in 2018. She was a Visiting Student with the Robert W. Galvin Center for Electricity Innovation, Illinois Institute of Technology, Chicago, USA. Her research interests include demand side management, smart grid modeling and control, and power system resilience.

**Wei Sun** received the Ph.D. degree in electrical engineering from Iowa State University, Ames, IA, USA, in 2011. He is currently an Assistant Professor with the Department of Electrical and Computer Engineering, University of Central Florida, Orlando, FL, USA. His research interests include power system restoration, smart grid operation and control, and cyber-physical system resilience, and security.

**Yifei Wang** received the M.Sc. degree in electrical engineering from Wuhan University, Wuhan, China, and the Ph.D. degree in electrical engineering from Zhejiang University, Hangzhou, China. He was a Post-Doctoral Fellow with the Electrical and Computer Engineering Department, Illinois Institute of Technology, Chicago, USA. He is currently an Assistant Professor with the School of Electrical Engineering, Southeast University, Nanjing, China. His research interests include convex optimization in power systems, power system operation, and economics. He serves as an Associate Editor for the *Journal of Modern Power Systems and Clean Energy*.

**Mohammad Shahidehpour** (F'01) received the Honorary Doctorate degree from the Polytechnic University of Bucharest, Bucharest, Romania. He is a University Distinguished Professor and serves as the Director of the Robert W. Galvin Center for electricity innovation, Illinois Institute of Technology. He is also a Research Professor with the Center of Research Excellence in Renewable Energy and Power Systems, King Abdulaziz University, Jeddah, Saudi Arabia. He was the recipient of the 2019 IEEE PES Ramakumar Family Renewable Energy Excellence Award. He is a member of the U.S. National Academy of Engineering.

**Zhiyi Li** (GSM'14–M'17) received the B.E. degree in electrical engineering from Xi'an Jiaotong University, Xi'an, China, in 2011, the M.S. degree from Zhejiang University, Hangzhou, China, in 2014, and the Ph.D. degree from the Illinois Institute of Technology in 2017, where he was a Senior Research Associate with the Robert W. Galvin Center for Electricity Innovation from August 2017 to May 2019. Since June 2019, he has been with the College of Electrical Engineering, Zhejiang University as a Tenure-Track Assistant Professor.

**Ciwei Gao** received the M.Eng. degree in electrical engineering from Wuhan University, Wuhan, China, in 2002, and the Ph.D. degree in electrical engineering from Shanghai Jiao Tong University, China, and Polytecnico di Torino, Italy, in 2006. He is currently a Professor with the School of Electrical Engineering, Southeast University, China. His research interests include electricity market, demand side management, and power system planning.